Scanning-probe-induced defects in thin SiO_2 film on Si: Comparison with Si clusters

Noriyuki Miyata
Advanced Semiconductor Research Center, National Institute of Advanced Industrial Science and Technology (ASRC, AIST), AIST Tsukuba Central 4, 1-1-1 Higashi, Tsukuba, Ibaraki 305-8562, Japan

Masakazu Ichikawa
Advanced Semiconductor Research Center, National Institute of Advanced Industrial Science and Technology (ASRC, AIST), AIST Tsukuba Central 4, 1-1-1 Higashi, Tsukuba, Ibaraki 305-8562, Japan
and Department of Applied Physics, The University of Tokyo, 7-3-1 Hongo, Bunkyo-ku, Tokyo 113-8656, Japan
(Received 14 October 2003; revised manuscript received 12 April 2004; published 13 August 2004)

We used scanning tunneling microscopy and spectroscopy to examine Si-clusterlike defects which were created by a scanning-probe-induced process around the intrinsic defects in a thermally grown SiO_2 film on Si. We compared these defects with Si clusters deposited on ultrathin Si oxide. Two types of defects were recognized, which have energy gaps at around 3.8 and 2.5 eV. We proposed that these two types of defects correspond to inner and surface damage on SiO_2 film.

DOI: 10.1103/PhysRevB.70.073306 PACS number(s): 68.37.Ef, 77.55.+f, 68.55.Ln, 81.65.Mq

The structural change of defects in thermally grown SiO_2 film on Si is of major concern in the reliability issue of metal oxide semiconductor devices.[1,2] Electron-spin-resonance and optical absorption studies showed that as-grown SiO_2 film contains oxygen-deficient-type defects (≡Si-Si≡).[3–5] It has been reported that charge trap around this type of defect leads to the formation of a pair of near sp^2 hybridized and sp^3 hybridized Si atoms or more complex transformation,[3,6,7] but the relationship with the electrical degradation of gate oxide is still controversial. Scanning tunneling microscopy (STM) and spectroscopy (STS) on the other hand have been used to separately investigate individual defects in thin oxide films. It has been reported that the scanning tunneling current of defect exhibits negative differential resistance or hump-shaped curve.[8–11] We recently reported that the development of scanning tunneling spectra occurs during the STS observation and proposed that intrinsic defects in thin oxide and oxynitride films (<0.7 nm) change to Si-clusterlike structures.[11] The identification of resultant defect structures is required to understand this probe-induced process in the film. However, the STM images of defects are somewhat indistinct, because of the overlap effect of surrounding SiO_2 network, so that we cannot directly discuss their structures from the STM images.

On the other hand, the energy gap E_g of the Si cluster depends on physical size because of carrier confinement, when the diameters become less than the free-exciton Bohr radius ($\sim$5 nm).[12–14] This implies that energy gaps are useful indicators for discussing the physical structures of probe-induced defects. In this work, we therefore compare the energy gaps of probe-induced defects in SiO_2 film with those of Si clusters by using STM and STS and discuss the defect structures.

The SiO_2 film was prepared on a *n*-type Si(001) substrate under ultrahigh vacuum (UHV) treatment and furnace oxidation. First, a clean Si(001)-2×1 surface was prepared by heating at 900 °C in the UHV. Second, an ultrathin Si oxide layer, about 0.3-nm thick, was thermally grown at 650 °C in 2×10^{-6} Torr O_2 for 10 min.[15] Finally, the sample was taken out from the vacuum chamber, and put into a quartz furnace. Furnace oxidation was carried out in 32% O_2 in Ar at atmospheric pressure at 700 °C for 900 s. The x-ray photoelectron spectroscopy observation for this sample surface proved that SiO_2 (Si 4+ component in Si 2*p* photoelectron spectrum) was the dominant chemical structure. We estimated the thickness to be 1.1 nm from the ratio of Si oxide and Si components in the Si 2*p* photoelectron spectrum.[11] We also prepared about 0.3-nm-thick Si oxide, 0.3-nm-thick Si oxynitride layers, and Si clusters. The 0.3-nm-thick oxide was grown under the same oxidation conditions as those above. The 0.3-nm-thick oxynitride was thermally grown on a clean Si(001)-2×1 surface at 650 °C in 2×10^{-6} Torr NO.[11] To prepare the Si clusters, silicon with the coverage of 0.12–0.38 monolayer (ML) was deposited on the 0.3-nm-thick oxide at 550 °C in a UHV ($<1\times10^{-9}$ Torr). These samples were observed by using an UHV-STM system with W tips prepared by electrochemical etching. The 1.1-nm-thick SiO_2 was carefully heated up to 350 °C in the UHV to remove the surface adsorbate before being examined. The 0.3-nm-thick oxide, oxynitride, and Si clusters were observed *in situ*.[11] The STM images were acquired at a sample bias (V) of +4.0 V with a tunnel current (I) of 30 pA. The I-V curves were measured by fixing the tip height for the same tunneling conditions as those of STM observation.

The STM image of the 1.1-nm-thick SiO_2 in Fig. 1(a) has a granular structure, meaning that the SiO_2 is amorphous. This result is consistent with the previous report on SiO_2 surface.[8] The dI/dV curve in Fig. 2(I), which was acquired from the area indicated by the arrow in Fig. 1(a), exhibits two sharp peaks at −3.8 and +3.6 V (energy gap=7.4 eV). For this structure, there are two candidate models which were reported to have 7.6 eV absorption band; oxygen vacancy (≡Si-Si≡) and complex defect containing a twofold-coordinated silicon.[5,16–19] Although it was purposed that the latter model contains impurity hydrogen and/or chlorine,[19] *in situ* STS observation for the ultrathin oxide and oxynitride

 ©2004 The American Physical Society

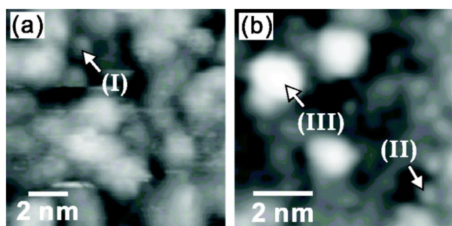

FIG. 1. STM images. (a) 1.1-nm-thick SiO_2. (b) Si clusters grown on 0.3-nm-thick Si oxide (0.25-ML Si deposition).

prepared in the UHV chamber also showed similar spectra with the gaps of about 7.4 eV. We therefore consider that the 7.4 eV gap observed in this work corresponds to the former structure. On the other hand, after three STS measurements, the spectrum of defect changes to a different type with broad states at both bias sides [Fig. 2(I) → Fig. 2(I′)]. We consider that this change corresponds to a structural change around the intrinsic ≡Si-Si≡ defect. More elaborate tracing is desired to understand the probe-induced process, but we could not access such an experiment, because the defect density was less than 1×10^{12} cm^{-2} and most defects (>90%) has already undergone transformation during STM observation before STS measurement. In this work, we therefore investigated the resultant structures to infer probe-induced process.

Let us turn to the Si clusters. The STM image for 0.25-ML Si deposition shown in Fig. 1(b) indicates that hemispherical Si clusters (bright spots) grew on the oxide.[20] The dI/dV curves of clusters in Figs. 2(II) and 2(III) have broad valence and conduction bands. The cluster density having this type spectrum increased to be 1.8×10^{13} cm^{-2} at 3.8-ML Si deposition, although the defect density in the oxide was less than 1×10^{12} cm^{-2}. In addition, the small clusters which have similar sizes to spots on the 0.3-nm-thick oxide (<1 nm in diameter) had larger energy gaps than defects in 0.3-nm-thick oxide, as we mentioned below. These results indicate that the defects in the oxide can be ignored on the energy gap estimation of Si clusters. Here, we assumed that the width between the edges of both states correspond to the

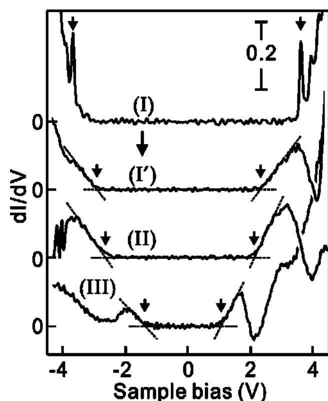

FIG. 2. STS (dI/dV) curves observed from defect in 1.1-nm-thick SiO_2 and Si clusters. (I) and (I′) are defects in SiO_2 indicated by arrow (I) in Fig. 1(a). (II) and (III) are Si clusters indicated by arrows (II) and (III) in Fig. 1(b).

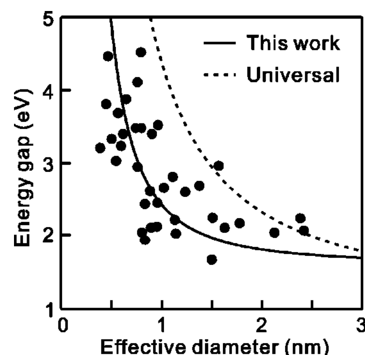

FIG. 3. Size dependence of energy gaps observed from Si clusters. Dotted curve indicates universal curve for crystal Si nanostructures (Refs. 23 and 24). Solid curve is present fitting curve expressed by Eq. (2).

energy gaps (Fig. 2). It is found that the bigger and smaller clusters, respectively, exhibit smaller and larger energy gaps, representing that the STS method can measure size-dependent energy gaps of Si clusters. It is also found that the dI/dV curves of clusters are quite similar to those of probe-induced defects, which suggest that the defects have Si-clusterlike electronic structures. Here, we should explain the effect of surface termination around the clusters. In previous studies using photoluminescence measurement, the surfaces of clusters were terminated with hydrogen or oxide, because the surface states caused nonradiative recombination centers.[14,21,22] In our research, the bottom side of the cluster is terminated with oxide, but the hemispherical surface probably remains nonterminated. To examine the termination effect on the size dependence, we prepared oxide-terminated Si clusters by exposing a Si-cluster-grown sample to 1200 L O_2 ($1\ \mathrm{L}=1\times10^{-6}$ Torr/s) at room temperature, and found a similar opening of energy gaps. These results indicate that the size effect takes place on both nonterminated and oxide-terminated clusters. On the other hand, it is expected that the surface oxide of clusters cause errors in determining cluster sizes from the STM images. In addition, the probe-induced defects likely have dangling bonds, since this process includes breakage of Si-O bonds. In this work, we therefore employ nonterminated clusters for comparison with probe-induced defects.

The idea of effective size parameters is helpful in comparing with Si nanostructures with different shapes. Zunger and Wang,[23] proposed an effective diameter D_{eff}, which was defined by the diameter of a sphere that had the same volume as a different-shaped structure. D_{eff} is given by $D_{\mathrm{eff}}=0.794D$ (nm) for the hemispherical shape of a cluster. Here, we assumed D to be the diameter of a cluster in the STM image. The solid circles for the experimental data in Fig. 3 show that the energy gaps increase with decreasing the effective diameters. The dotted curve, which was proposed by using an empirical pseudopotential calculation,[23,24] is expressed as

$$E_g = 1.17 + 3.3D_{\mathrm{eff}}^{-1.37}, \tag{1}$$

where 1.17 corresponds to the energy gap of bulk crystalline Si. The optical gaps experimentally measured from Si clus-

ters and tight-binding calculation were approximately consistent with this curve,[22,25] so that Eq. (2) is regarded to be a universal curve for Si nanostructures. Our experimental date also roughly agrees with the universal curve, but most of the data is slightly smaller than this. We first considered that this discrepancy is related to the assumption of effective diameter. Actually, it was reported that the energy gap of extremely elongated box shape is larger than that of cubic shape with the same volume, while small shape difference does not affect the energy gaps.[23] However, our result showed opposite tendency, namely, the hemispherical clusters showed smaller energy gaps than the universal curve, so we ignored the effect of shape difference on the discussion of Si clusters. We presently considered that the surface states affect carrier confinement,[26] since the clean Si surface remains on the hemispherical cluster surface. In addition, we have to take the effect of disordered structures into account.[27] Although epitaxial Si clusters usually grow at 550 °C because the ultrathin Si oxide partially decomposes,[21] it is expected that, at small Si coverage (<1 ML), nonepitaxial clusters remain on the oxide surface. The solid curve in Fig. 3 is the best fitting, which is given by

$$E_g = 1.6 + 0.8D_{\mathrm{eff}}^{-2}. \qquad (2)$$

The fitted energy gap of 1.6±0.4 eV and exponent of 2±0.5 are approximately consistent with those reported on amorphous Si clusters expressed as $E_g=1.56+2.4D^{-2}$ (eV).[27] This result suggests that the deposited Si clusters contain disordered structures. On the other hand, the fitted confinement parameter of 0.8±0.4 is smaller than that of the amorphous Si clusters, indicating the reduction of electron and hole effective masses. We consider that the surface states around the clusters reduce the effective masses. Incidentally, the large errors in the fitting parameters reflect large dispersion of experimental data around the fitting curve. This is likely to indicate that clusters have varieties of structural disorders and surface states.

Let us next return to probe-induced defects. The energy gap distribution for defects in the 1.1-nm-thick SiO_2 shown in Fig. 4(a) exhibits two distinct parts with a main peak at 3.8±0.1 eV and a weak peak at 2.5±0.2 eV. We therefore divide the defect structures into two types. Figure 4(b) shows that the high-energy part approximately disappears in the 0.3-nm-thick Si oxide. The 0.3-nm-thick oxide corresponds to the oxidation of about one monolayer of Si on a Si(001) surface,[28] indicating that a complete SiO_2 network is not formed in this layer. These results suggest that the high-energy part corresponds to the structure created in the SiO_2 film, namely, structural transformation occurs around the ≡Si-Si≡ that is in the SiO_2 network. On the other hand, we can expect that probe-induced defects would have some disorders, since they were created in amorphous oxide at room temperature. In addition, dangling bonds likely remain in the defects. Therefore, the solid curve in Fig. 3 is an appropriate curve for roughly estimating the defect sizes. We calculated the effective diameter for the high-energy gap to be 0.6±0.02 nm from Eq. (2). Here, the numbers of Si atoms N_{Si} in the cluster are approximately given by $N_{\mathrm{Si}}=26.1D_{\mathrm{eff}}^3$ (atom), so that this inner defects contains about 5–7 Si atoms. These results indicate that the probe-induced damage affects at least second neighboring Si atoms around the ≡Si-Si≡.

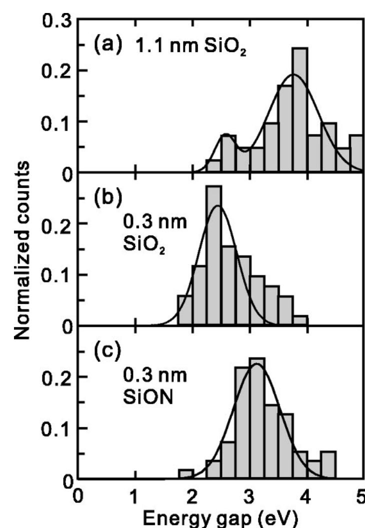

FIG. 4. Distributions of energy gaps observed from defects. (a) 1.1-nm-thick SiO_2. (b) 0.3-nm-thick Si oxide. (c) 0.3-nm-thick Si oxynitride.

The structure for the low-energy part at around 2.5 eV likely corresponds to damage around the SiO_2 surface or SiO_2/Si interface, because the major defects in 0.3-nm-thick oxide are this type of structure. The energy gap distribution for the 0.3-nm-thick oxynitride in Fig. 4(c) indicates a shift toward a higher energy than that for the 0.3-nm-thick oxide, representing that the nitrogen in the layer affects the probe-induced process. If damage develops from the oxide/Si interface to the Si substrate, it is likely that nitrogen would be ineffectual on damaging process. We therefore consider that the low-energy part corresponds to damage around the oxide surface. From Eq. (2), effective diameters for the peak energies of ultrathin oxide and oxynitride are calculated to be about 1.0±0.15 nm (16–40 Si atoms) and 0.7±0.05 nm (7–11 Si atoms), respectively. It is obvious that the calculated size for the ultrathin oxide is too large, if spherical structures are created in the layer. We consider that the shape of surface defect is not a complete sphere, but disklike structures around the surface. Furthermore, if much dangling bonds remain in these structures, the energy gaps would be reduced compared with the inner defects. These two effects likely lower the energy gaps of surface defects. From the above discussion, we propose that the probe-induced process produces inner and surface defective structures on furnace-grown SiO_2 film.

It was proposed that charge-induced structural change leads to the breakage of a single Si-Si bond.[6] A slightly complex model was also proposed, but the network movement is limited around the Si-Si dimmer structure.[7] Comparing these models, probe-induced damage observed in this work is obviously a large structural change, even though intrinsic defect is embedded in the SiO_2 network. Similar network damage has been reported for vacuum ultraviolet irradiation to SiO_2, where oxygen atoms are removed from the network.[29] A similar reaction probably occurs in the probe-induced pro-

cess. On the other hand, Lombardo *et al.* recently reported that a threshold voltage of about 4 V appears during the growth of breakdown spots in very thin gate SiO_2 film (1.5–2.25 nm).[30] We consider that this phenomena is related to the inner defects observed in this work. If further damaging around the inner defects requires excitation of this structure (~3.8 eV), a threshold voltage is likely to occur at around 4 V. We consider that a Si-clusterlike defect with a diameter of about 0.6 nm is created as a metastable structure during the electrical breakdown of thin SiO_2 film.

In summary, the probe-induced structural change around the Si-Si bond in the SiO_2 leads to two types of defective structures. We proposed that one is an inner defect with an energy gap of about 3.8 eV. We roughly estimated the effective diameter of this type defect to be 0.6 nm. The other is a slightly larger defective structure created around the SiO_2 surface with an energy gap of about 2.5 eV.

This work was supported by the New Energy and Industrial Technology Development Organization (NEDO).

[1] M. L. Green, E. P. Gusev, R. Degraeve, and E. L. Garfunkel, J. Appl. Phys. **90**, 2057 (2001).
[2] J. H. Stathis, IBM J. Res. Dev. **46**, 265 (2002).
[3] H. S. Witham and P. M. Lenahan, Appl. Phys. Lett. **51**, 1007 (1987).
[4] W. L. Warren, P. M. Lenahan, and C. J. Brinker, J. Non-Cryst. Solids **139**, 151 (1991).
[5] N. Terada, T. Haga, N. Miyata, K. Moriki, M. Fujisawa, M. Morita, T. Ohmi, and T. Hattori, Phys. Rev. B **46**, 2312 (1992).
[6] J. W. McPherson, V. K. Reddy, and H. C. Mogul, Appl. Phys. Lett. **71**, 1101 (1997).
[7] Z.-Y. Lu, C. J. Nicklaw, D. M. Fleetwood, R. D. Schrimpf, and S. T. Pantelides, Phys. Rev. Lett. **89**, 285505 (2002).
[8] M. Tabe and M. Tanimoto, Appl. Phys. Lett. **58**, 2105 (1991).
[9] H. Watanabe, T. Baba, and M. Ichikawa, J. Appl. Phys. **85**, 6704 (1999).
[10] J. Y. Park, R. J. Phaneuf, and E. D. Williams, J. Vac. Sci. Technol. B **19**, 523 (2001).
[11] N. Miyata and M. Ichikawa, Jpn. J. Appl. Phys., Part 2 **40**, L1271 (2001); J. Appl. Phys. **92**, 1850 (2002).
[12] B. Delley and E. F. Steigmeier, Phys. Rev. B **47**, 1397 (1993).
[13] C. Delerue, G. Allan, and M. Lannoo, Phys. Rev. B **48**, 11 024 (1993).
[14] D. J. Lockwood, Solid State Commun. **92**, 101 (1994).
[15] N. Miyata, H. Watanabe, and M. Ichikawa, Phys. Rev. Lett. **84**, 1043 (2000).
[16] E. P. O'Reilly and J. Robertson, Phys. Rev. B **27**, 3780 (1983).
[17] R. Tohmon, H. Mizuno, Y. Ohki, K. Sasagane, K. Nagasawa, and Y. Hama, Phys. Rev. B **39**, 1337 (1989).
[18] L. Skuja, J. Non-Cryst. Solids **149**, 77 (1992).
[19] A. N. Trukhin, L. N. Skuja, A. G. Boganov, and V. S. Rudenko, J. Non-Cryst. Solids **149**, 96 (1992).
[20] A. A. Shklyaev and M. Ichikawa, Phys. Rev. B **65**, 045307 (2001).
[21] T. van Buuren, L. N. Dinh, L. L. Chase, W. J. Siekhaus, and L. J. Terminello, Phys. Rev. Lett. **80**, 3803 (1998).
[22] L. Patrone, D. Nelson, V. I. Safarov, M. Sentis, and W. Marine, J. Appl. Phys. **87**, 3829 (2000).
[23] A. Zunger and L. Wang, Appl. Surf. Sci. **102**, 350 (1996).
[24] L. Wang and A. Zunger, J. Chem. Phys. **100**, 2394 (1994).
[25] S. G. Allan, Y. M. Niquet, and C. Delerue, Appl. Phys. Lett. **77**, 639 (2000).
[26] J.-B. Xia, and K. W. Cheah, Phys. Rev. B **59**, 14 876 (1999).
[27] N.-M. Park, C.-J. Choi, T.-Y. Seong, and S.-J. Park, Phys. Rev. Lett. **86**, 1355 (2001).
[28] H. Watanabe, N. Miyata, and M. Ichikawa, in *Fundamental Aspects of Silicon Oxidation*, edited by Y. J. Chabal (Springer, Berlin, 2001), p. 89.
[29] V. V. Afanas'ev, J. M. M. de Nijs, P. Balk, and A. Stesmans, J. Appl. Phys. **78**, 6481 (1995).
[30] S. Lombardo, J. H. Stathis, and B. P. Linder, Phys. Rev. Lett. **90**, 167601 (2003).